2nd URSI AT-RASC, Gran Canaria, 28 May – 1 June 2018

Effect of Element Pattern Symmetry on the Performance of Dual-Polarized GNSS Adaptive Antenna Arrays

Navid Rezazadeh* (1) and Lotfollah Shafai (1)
(1) Department of Electrical and Computer Engineering, University of Manitoba, Winnipeg, MB, Canada R3T5V6
(email: rezazadn@myumanitoba.ca; lot.shafai@umanitoba.ca)

Abstract

The effect of the element pattern symmetry on the performance of a two-element dual-polarized array for the interference suppression in GNSS is studied theoretically through Monte Carlo simulations of the array in the presence of interferers. It is shown that for most interference scenarios, the array of circular microstrip antennas performs the same as a four-element right-hand circularly-polarized (RHCP), despite occupying half the size. It is however shown that the capability of the dual-polarized array in suppressing RHCP interferers is limited when the array element patterns are equalized in the E- and H-planes.

1. Introduction

It is known that a receiver antenna for the global navigation satellite system (GNSS) has to be right-hand circular polarized (RHCP) with a low axial ratio. For microstrip antennas, pattern equalization in the E- and H-plane is necessary in ensuring a low axial ratio.

The receivers with a single antenna element are vulnerable to interference due to the low power level of the satellite signals [1]. Adaptive antenna arrays are then utilized to add the beamforming and null-steering capability to the receiver, to make them resilient in interference scenarios. It is desired that such antenna elements are physically small and have reasonable performance against interference [2]. Most of the arrays designed in the recent years consist of miniaturized RHCP microstrip antenna elements placed in a dense array with element spacings as small as $0.2\ \lambda_0$ [3].

It is known that an array of N RHCP elements provides $N-1$ degrees of freedom for beamforming. It is also known that an array of N dual-polarized elements has $2N-1$ degrees of freedom [4], therefore, such an array would require less number of elements compared to an RHCP array, for the same number of degrees of freedom. For instance, an array of two dual-polarized elements has three degrees of freedom, and is a more compact alternative to a four-element RHCP array. It is also known that a dual-polarized array can receive a desired signal even if an interferer incident angle is very close to that of the desired signal's, provided that their polarizations do not match [5].

Despite the apparent benefits of the dual-polarized arrays, only a few designs have been reported for the GNSS applications [6]-[9]. The goal of this work is to verify the capability of the dual-polarized arrays, as well as their possible limitations.

To this end, we consider an array of two dual-polarized antenna elements and evaluate its performance through many Monte Carlo simulations of various interference scenarios, and compare it to the performance of an array of four RHCP elements. The array geometries and element radiation patterns are given in section 2 and the array performance evaluation is presented in section 3.

2. Array Geometry and Element Patterns

The two array geometries to be studied are shown in Figure 1. We assume the inter-element spacing in both arrays is $d = 0.25\ \lambda_0$.

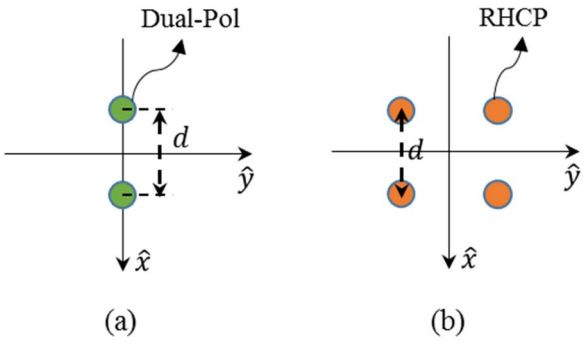

Figure 1. The array configurations considered in this work. (a) An array of two dual-polarized antenna elements. (b) An array of four RHCP antenna elements.

The radiation pattern of an x-polarized circular microstrip antenna is

$$\vec{E}(\theta,\varphi) = f(\theta)\cos\varphi\,\hat{\theta} + g(\theta)\sin\varphi\,\hat{\phi} \qquad (1).$$

where the functions $f(\theta)$ and $g(\theta)$ determine the radiation pattern in the E- and H- planes. We consider two cases for these functions. First, assuming the antenna is printed on a thin substrate with infinite ground plane, we have [10]

$$\begin{cases} f(\theta) = [J_2(k_0 a \sin\theta) - J_0(k_0 a \sin\theta)] \\ g(\theta) = [J_2(k_0 a \sin\theta) + J_0(k_0 a \sin\theta)] \cos\theta \end{cases} \quad (2).$$

in which J_n is the Bessel function of the first kind, k_0 is the propagation constant in free space and a is the patch radius. Assuming a dielectric constant of $\epsilon_r = 25$, the patch radius is approximately $0.05\,\lambda_0$, and the radiation patterns are shown in Figure 2 (a). The E- and H- plane patterns are not equal in this case. To achieve an RHCP pattern for this antenna, a y-polarized pattern which can be found by $\vec{E}(\theta, \varphi - \pi/2)$ is added to the x-polarized pattern with a quadrature phase difference ($e^{-j\pi/2}$). The resulting CP patterns are given in Figure 1 (b), showing some cross-polarization at off-zenith angles due to the unequal E- and H-plane patterns of the linearly-polarized antenna.

For the second case, we consider $f(\theta) = -g(\theta) = 1$, which results in completely equalized E- and H-plane patterns as shown in Figure 2 (c). The corresponding CP patterns are shown in Figure 2 (d), showing a zero LHCP component, which is a result of the perfect pattern equalization. Note that the antenna does not radiate in the lower hemisphere.

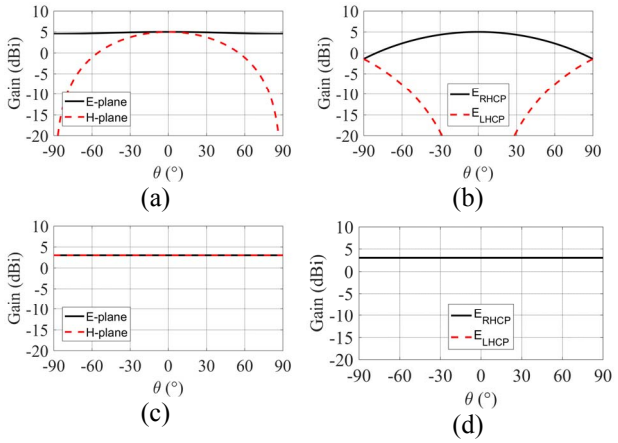

Figure 2. The element radiation patterns. (a) An x-polarized disk patch antenna on an infinite ground plane. (b) An isotropic x-polarized antenna. (c) An RHCP disk patch antenna on an infinite ground plane. (d) An isotropic RHCP antenna.

3. Array Performance Evaluation

3.1 Method

To evaluate the performance of the antenna arrays, it is assumed that the arrays are connected to a four-channel signal processing unit, ignoring the effects of the RF front-ends. 100 Monte Carlo simulations with random interference angles are run. In each simulation, we assume that several interferers are incident from 0° to 30° elevation angle, and a desired signal whose incident angle is swept in the upper hemisphere. For each interference scenario, the signals received by the array channels are multiplied by a complex weight vector $\mathbf{w} = [w_1\ w_2\ w_3\ w_4]^T$, which is found by power minimization method with a linear constraint $\mathbf{c}$ as [11]

$$\mathbf{w}_{opt} = \frac{\boldsymbol{R}_x^{-1}\mathbf{c}}{\mathbf{c}^H \boldsymbol{R}_x^{-1}\mathbf{c}} \quad (3).$$

in which $\mathbf{R}_x = E\{\mathbf{x}\mathbf{x}^H\}$ is the covariance matrix of the received signal. Assuming that the desired signal, interference signals and noise are uncorrelated, the signal-to-interference-and-noise ratio (SINR) at the output of the processor is

$$\mathrm{SINR}_{\mathrm{out}} = \frac{\mathbf{w}_{opt}{}^H \mathbf{R}_d \mathbf{w}_{opt}}{\mathbf{w}_{opt}{}^H (\mathbf{R}_i + \mathbf{R}_n) \mathbf{w}_{opt}} \quad (4).$$

in which $\mathbf{R}_d$, $\mathbf{R}_i$, $\mathbf{R}_n$ are the covariance matrix of the desired signal, interference and noise respectively, given by

$$\begin{cases} \mathbf{R}_d = \mathbf{u}_d P_d \mathbf{u}_d{}^H \\ \mathbf{R}_i = \sum \mathbf{u}_i P_i \mathbf{u}_i{}^H \\ \mathbf{R}_n = P_n \mathbf{I}_N \end{cases} \quad (5).$$

where $\mathbf{u}_d$ and $\mathbf{u}_i$ are the array response to the desired and interfering signals respectively, and P_d, P_i and P_n are the desired signal, interference and noise powers at the input of an isotropic element. We assume $P_d/P_n = -20\,dB$ and $P_i/P_n = 20\,dB$.

3.1 Results

The results of the Monte Carlo simulations are presented in this section. The constraint vector considered for the power minimization method is $\mathbf{c} = [1\ 0\ 0\ 0]^T$ for the RHCP array and $\mathbf{c} = [1\ j\ 0\ 0]^T$ for the dual-polarized array.

Figure 3 shows the angular available space for reception, which is defined as the portion of the upper hemisphere where a desired signal could be received with an output SINR exceeding a threshold value $\mathrm{SINR}_{\mathrm{th}}$. The availability is shown as a function of the number of interferers, for two fixed values of the $\mathrm{SINR}_{\mathrm{th}}$. Figure 3 (a) shows the performance of the arrays when the interferers are assumed to be RHCP, and Figure 3 (b) shows the performance when the interferers are assumed to be randomly-polarized.

It can be seen that for the case of randomly-polarized interferers, the two-element dual-polarized array performs similar to the four-element RHCP array and can suppress up to three interferers, for both cases of equalized and unequal element radiation patterns. The situation is however different for the case of RHCP interferes, where the dual-polarized array of the elements with equalized radiation patterns is not capable of using its degrees of freedom effectively and can only suppress one RHCP interferer. Therefore, the pattern equalization seems to be an undesirable feature for a dual-polarized array when suppressing RHCP interferers.

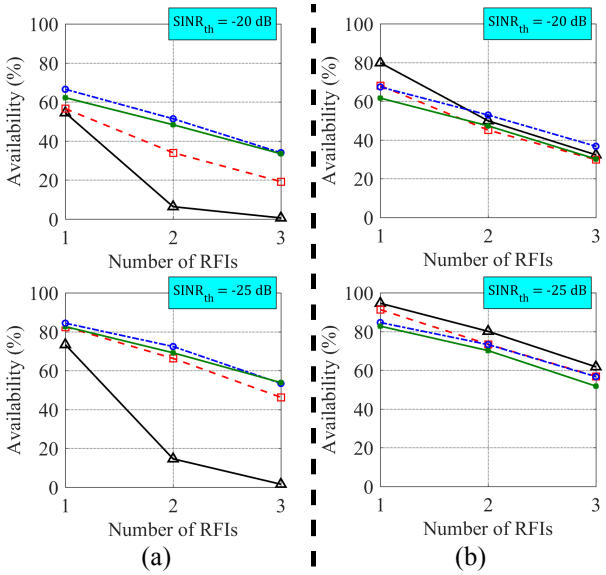

Figure 3. The angular availabilty as a function of the number of interferers, for two fixed values of the $SINR_{th}$. (a) The case of RHCP interferers. (b) The case of randomly-polarized interferers.

4. Conclusion

It was demonstrated that the performance of a dual-polarized antenna array in the presence of RHCP interferers is strongly affected by the equalization of the pattern in the E- and H-planes. It was shown that, as opposed to the RHCP arrays where element pattern equalization is desirable for low axial ratio, it limits the effective number of RHCP interferers a dual-polarized array can suppress. Additional theoretical and measurement results will be presented at the conference.

5. References

1. C. Fernández-Prades, J. Arribas and P. Closas, "Robust GNSS Receivers by Array Signal Processing: Theory and Implementation," in *Proceedings of the IEEE*, vol. 104, no. 6, pp. 1207-1220, June 2016. doi: 10.1109/JPROC.2016.2532963.

2. I. J. Gupta, I. M. Weiss and A. W. Morrison, "Desired Features of Adaptive Antenna Arrays for GNSS Receivers," in *Proceedings of the IEEE*, vol. 104, no. 6, pp. 1195-1206, June 2016. doi: 10.1109/JPROC.2016.2524416

3. J. L. Volakis, A. J. O'Brien and C. C. Chen, "Small and Adaptive Antennas and Arrays for GNSS Applications," in *Proceedings of the IEEE*, vol. 104, no. 6, pp. 1221-1232, June 2016, doi: 10.1109/JPROC.2016.2528165.

4. R. L. Fante, "Principles of adaptive space-time-polarization cancellation of broadband interference." In *ION GNSS*, pp. 584-591. 2004.

5. R. Compton, "On the performance of a polarization sensitive adaptive array," in *IEEE Transactions on Antennas and Propagation*, vol. 29, no. 5, pp. 718-725, Sep 1981. doi: 10.1109/TAP.1981.1142651

6. E. C. Ngai, D. J. Blejer, Tri Phuong and J. Herd, "Anti-jam performance of small GPS polarimetric arrays," *IEEE Antennas and Propagation Society International Symposium (IEEE Cat. No.02CH37313)*, 2002, pp. 128-131 vol.2. doi: 10.1109/APS.2002.1016044

7. M. Trinkle, and W. C. Cheuk. "Null-steering GPS dual-polarized antenna arrays." In *Proceedings of the 6th International Symposium on Satellite Navigation Technology including Mobile Positioning and Location Services (SatNav'03)*. 2003.

8. W. C. Cheuk, M. Trinkle, and D. A. Gray. "Null-steering LMS dual-polarised adaptive antenna arrays for GPS." *Positioning*1, no. 09 (2005), 0.

9. W. Alshrafi, U. Engel and T. Bertuch, "Compact controlled reception pattern antenna for interference mitigation tasks of global navigation satellite system receivers," in *IET Microwaves, Antennas & Propagation*, vol. 9, no. 6, pp. 593-601, 4 24 2015. doi: 10.1049/iet-map.2014.0357

10. A. Derneryd, "Analysis of the microstrip disk antenna element," in *IEEE Transactions on Antennas and Propagation*, vol. 27, no. 5, pp. 660-664, September 1979. doi: 10.1109/TAP.1979.1142159

11. R. A. Monzingo and T. W. Miller, Introduction to Adaptive Arrays. New York Wiley, 1980.